Supplementary material

Supplementary methods — The average cortical response to oriented stimuli

Primary visual cortex responds strongly to grating stimuli with a well tuned, large differential response over the orientation of the stimuli. The resulting single-condition maps have a high signal to noise ratio, facilitating the location of active regions of cortex. For this reason we investigated the organisation of the cortical encoding of orientation, as opposed to other variables of the visual cortical representation, and restricted our stimuli to vary a single functional component: namely, the orientation of a set of edges. However, we assumed that once the baseline "blank" response has been subtracted, the cortical response to individual stimuli is independent, and that there is no preferred cortical response to oriented stimuli in general. If the cortex responded much more strongly to oriented stimuli in some regions, the single-condition snapshots of the cortical response would be corrupted by this "fixed pattern" noise. In that case, our active region location procedure could be biased towards a static, global state, and potentially distort our measurements of the spatial configuration of single OI response maps.

To examine this issue, we searched for areas over the cortical surface that were significantly more active on average, over all oriented stimuli. We divided the recordings of OI maps into several blocks, where one block contained a single presentation of each of the stimuli. For each block, we extracted single condition maps for each stimulus as described above. We then computed the average cortical activation for each block, over all single condition maps. Over the set of blocks comprising a single experiment, we computed which pixels on the map had a greater average activity than the mean activity taken over the entire imaged map. We used Student's t-test for significance, with a Holm-Bonferroni correction for multiple comparisons.

We performed this analysis in 18 cats, and found no evidence for a preferred orientation response in visual cortex. This implies that the average response near a pinwheel region is equal to the mean response of an iso-orientation domain, although the variance of the domain response is greater. There is also no conflict with the existence of regions of elevated cytochrome-oxidase activity (CO blobs) in V1 of macaque monkey, since any static activity pattern of CO regions would be subtracted along with the unstimulated ("blank") cortical response.

Supplementary tables

Source figure reference	Tracer used		Injected layers
Rockland and Lund 1983 Figure 10a.	HRP	(B)	Layers 2 and 3
Malach et al. 1993 Figures 2, 3.	biocytin	(A)	Not stated
Amir et al. 1993 Figures 4, 8.	biocytin	(A)	Superficial (200–600 μm depth)
Lund et al. 1993 Figure 9a, 9b, 9c, 9d. (9b shown in our Figure S1)	biocytin	(B)	Layers 2 and 3
Yoshioka et al. 1996 Figures 5, 6, 8, 10.	biocytin	(B)	Layers 2 and 3
Tanigawa et al. 2005 Figures 6a, 6b, 6c, 6d, 6e, 6f. (6b shown in our Figure S3)	BDA	(A)	Layer 3

Supplementary Table 1: Figures used for anatomical analysis of the superficial patch system (macaque monkey V1). Injections were included when they were confined to a single cortical area, and no simultaneous injection was made into another cortical area. Many tracers are not restricted to unidirectional tracer transport, especially when large pressure injections are made. For this reason, no attempt was made to distinguish between anterograde and retrograde labelling, unless retrograde-only labelling was reconstructed by the original researchers. Nevertheless, when the referenced papers stated that they observed or reconstructed pure retrograde (R), pure anterograde (A) or bi-directional (B) transport, this has been noted above. Only figures that showed reconstructions of photomicrographs, made in tangential section through the superficial layers only, where the original authors had delineated patch boundaries were included, or where clusters of retrogradely-labelled cells were visible. The figures listed here represent 27 injections made into macaque monkey V1.

Source figure reference	Tracer used		Injected layers
Gilbert and Wiesel 1989, Figures 5b, 5c.	latex microspheres	(R)	Layers 3/4 border (500–600 μm)
Callaway and Katz 1990, Figure 6a.	latex microspheres	(R)	Columnar, spanning cortex
Luhmann et al. 1990, Figure 7d.	HRP	(B)	Superficial (500 μm)
Callaway and Katz 1991, Figures 1a, 1b.	latex microspheres	(R)	Columnar, spanning cortex
Lübke and Albus 1992, Figures 2a, 2b.	HRP	(R)	Layers 1–4
Kisvárday and Eysel 1992, Figure 3a.	biocytin	(B)	Layer 3
Kisvárday et al. 1997, Figure 7i. (Shown in our Figure S2)	biocytin	(A)	Layers 3–4 (300–600 μm)
Schmidt et al. 1997, Figures 2a, 2b.	latex microspheres	(R)	Not stated
Buzás et al. 2006, Figure 5a.	biocytin	(A)	Superficial (300–400 μm)

Supplementary Table 2: Figures used for anatomical analysis of the superficial patch system (cat area 17). Criteria for including injections were identical to those described in Table ST1. The figures listed here represent 13 injections made into cat area 17.

Supplementary figures

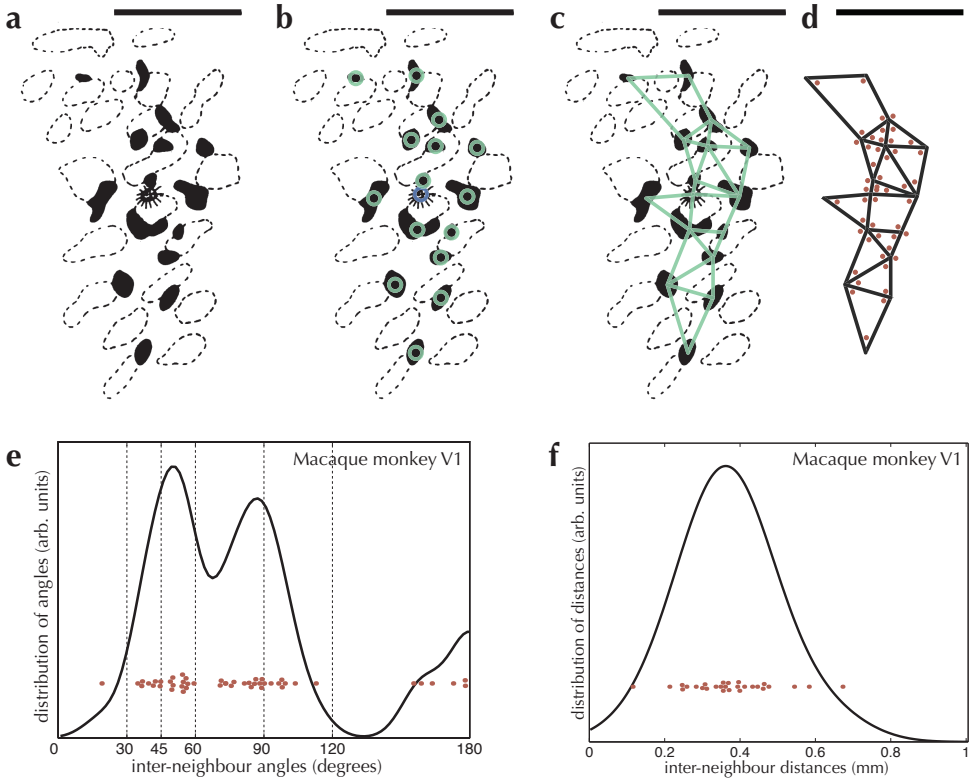

Supplementary Figure 1: Analysis of an injection of biocytin made into layers 2 and 3 of macaque monkey V1 (area 17) (Lund et al. 1993). **a** Reproduction of Figure 9b of Lund et al. 1993, showing patches of axonal terminals (black regions) labelled from an injection of biocytin (fringed stippled area), as well as CO-rich domains (regions with dashed borders). **b** The locations of labelled patches and of the injection site were taken as the centre of mass of each of the labelled regions. **c** A graph connecting neighbouring locations was constructed using a Gabriel-graphing analysis (see Methods for more details). **d** All interior angles formed by the neighbour graph were collected as a statistical measure for the shape of the neighbour graph. Collected angles are marked with brown dots in **d**–**e**. The distribution of angles shown as the black curve in **e** was estimated by summing Gaussian kernels of width 8 degrees (98% of the kernel weight) placed at each observation (brown dots). The distribution of distances between neighbouring patches (**f**) was likewise estimated using a Gaussian kernel of 100 µm width. Scale bars: 1 mm in **a**–**d**. Parts **a**–**c** reproduced with permission from Oxford University Press.

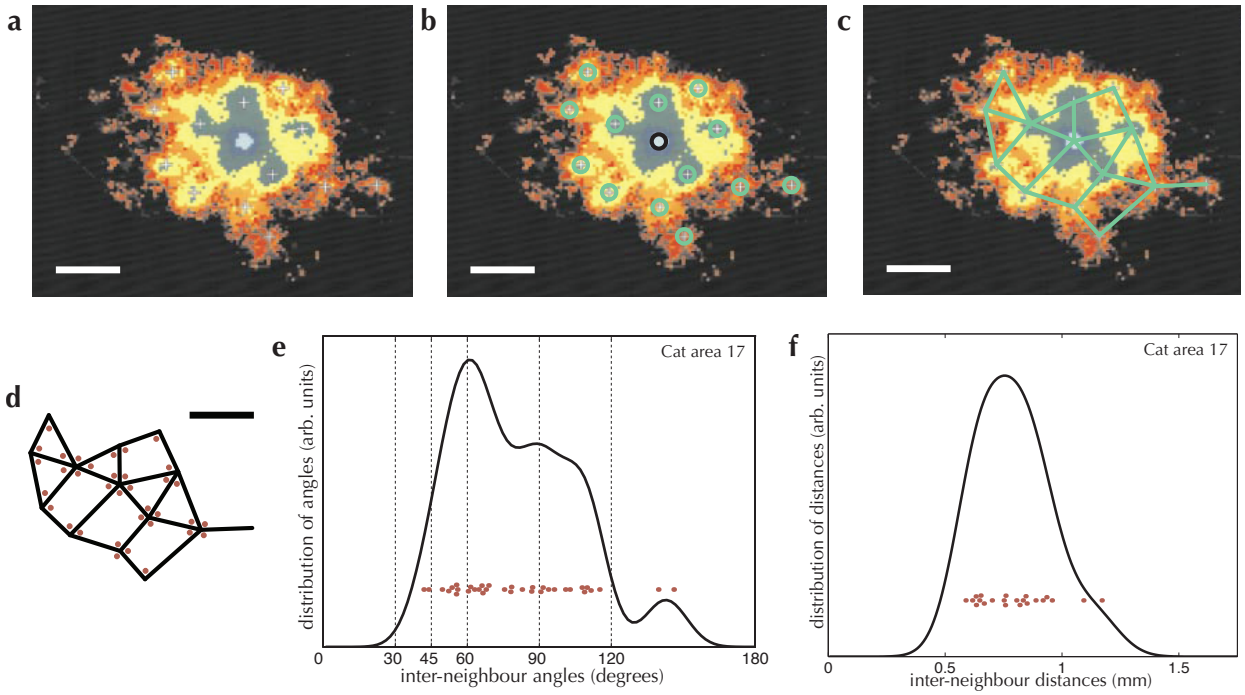

Supplementary Figure 2: Analysis of an injection of biocytin made into layers 3 and 4 of cat area 17 (Kisvárday et al. 1997). **a** Reproduction of figure 7i of Kisvárday et al. 1997, showing clustering in the density pattern of labelled excitatory boutons, produced by the injection at the centre of the figure. Marked peaks in density (white crosses in **a**–**b**) were identified as patches by the original investigators. These locations were used by us for further analysis (**b**–**f**), and were considered to be the centres of patches. Other conventions are as in Figure S1. Scale bars: 1 mm in **a**–**d**. Parts **a**–**c** reproduced with permission from Oxford University Press.

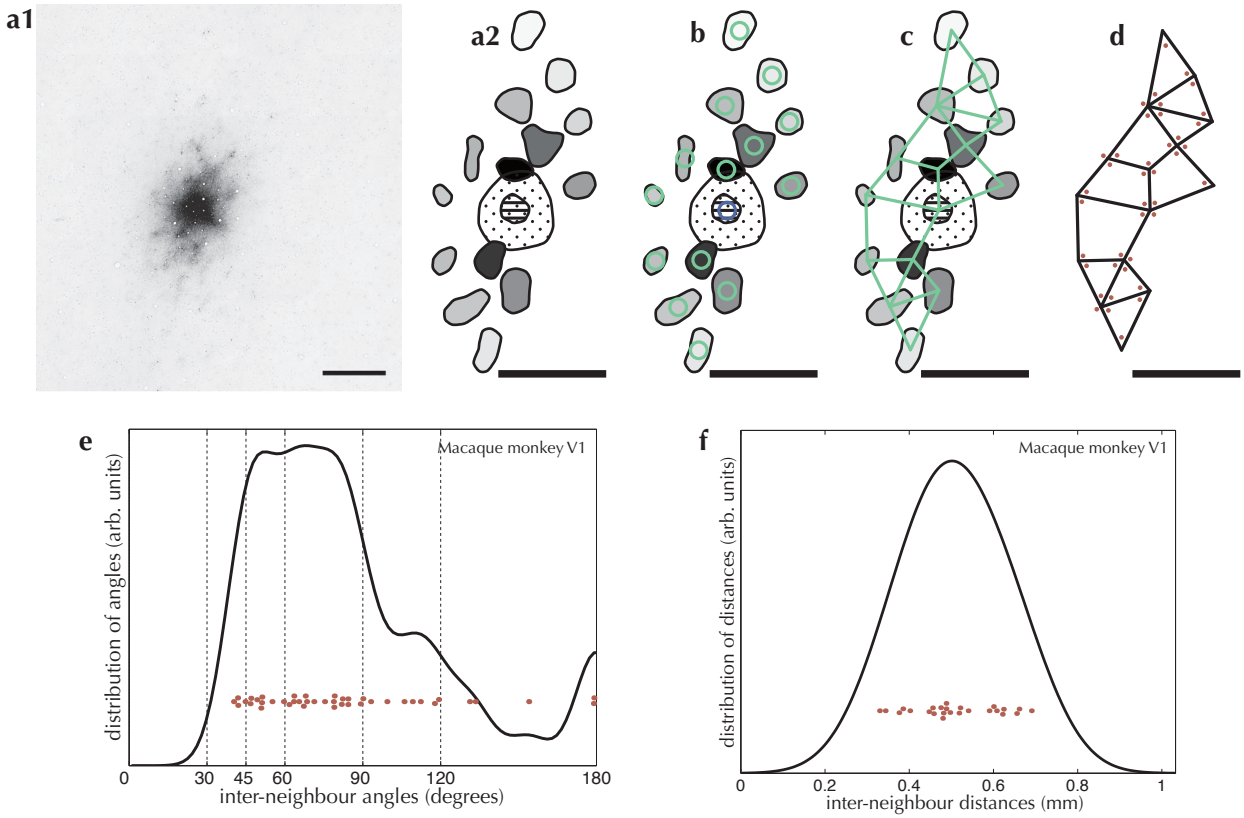

Supplementary Figure 3: Analysis of a 250 µm diameter injection of BDA made into layer 3 of macaque monkey V1 (area 17) (Tanigawa et al. 2005). **a1** Reproduction of figure 5a of Tanigawa et al. 2005, showing a photomicrograph of the BDA injection and surrounding labelling, in tangential section. **a2** Redrawn figure 6b of Tanigawa et al. 2005, showing the labelled patches identified by the original investigators, for the injection shown in **a1**. These regions were used by use for further analysis (**b**–**f**), by taking the patch location as the centre of mass of each labelled region. Other conventions are as in Figure S1. Scale bars: 1 mm in **a**–**d**. Parts **a**–**c** reproduced with permission from Oxford University Press. Parts **a2**–**c** redrawn from Tanigawa et al. 2005.

Supplementary references

Amir Y, Harel M, Malach R. 1993. Cortical Hierarchy Reflected in the Organization of Intrinsic Connections in Macaque Monkey Visual Cortex. J Comp Neurol, 334:19-46.

Buzás P, Kovács K, Ferecskó AS, Budd JML, Eysel UT, Kisvárday ZF. 2006. Model-based analysis of excitatory lateral connections in the visual cortex. J Comp Neurol, 499:861-881.

Callaway EM, Katz LC. 1990. Emergence and refinement of clustered horizontal connections in cat striate cortex. J Neurosci, 10:1134-1153.

Callaway EM, Katz LC. 1991. Effects of binocular deprivation on the development of clustered horizontal connections in cat striate cortex. Proc Natl Acad Sci USA, 88:745-749.

Gilbert CD, Wiesel TN. 1989. Columnar specificity of intrinsic horizontal and corticocortical connections in cat visual cortex. J Neurosci, 9:2432-2442.

Kisvárday ZF, Eysel UT. 1992. Cellular organization of reciprocal patchy networks in layer III of cat visual cortex (area 17). Neuroscience, 46:275-286.

Kisvárday ZF, Tóth É, Rausch M, Eysel UT. 1997. Orientation-specific relationship between populations of excitatory and inhibitory lateral connections in the visual cortex of the cat. Cereb Cortex, 7:605-618.

Lübke J, Albus K. 1992. Lack of exuberance in clustered intrinsic connections in the striate cortex of one-month-old kitten. Eur J Neurosci, 4:189-192.

Luhmann HJ, Singer W, Martinez-Millán L. 1990. Horizontal interactions in cat striate cortex: I. Anatomical substrate and postnatal development. Eur J Neurosci, 2:344-357.

Lund JS, Yoshioka T, Levitt JB. 1993. Comparison of intrinsic connectivity in different areas of macaque monkey cerebral cortex. Cereb Cortex, 3:148-162.

Malach R, Amir Y, Harel M, Grinvald A. 1993. Relationship between intrinsic connections and functional architecture revealed by optical imaging and in vivo targeted biocytin injections in primate striate cortex. Proc Natl Acad Sci USA, 90:10469-10473.

Rockland KS, Lund JS. 1983. Intrinsic laminar lattice connections in primate visual cortex. J Comp Neurol, 216:303-318.

Schmidt KE, Goebel R, Löwel S, Singer W. 1997. The perceptual grouping criterion of colinearity is reflected by anisotropies of connections in the primary visual cortex. Eur J Neurosci, 9:1083-1089.

Tanigawa H, Wang Q, Fujita I. 2005. Organization of Horizontal Axons in the Inferior Temporal Cortex and Primary Visual Cortex of the Macaque Monkey. Cereb Cortex, 15:1887-1899.

Yoshioka T, Blasdel GG, Levitt JB, Lund JS. 1996. Relation between patterns of intrinsic lateral connectivity, ocular dominance, and cytochrome oxidase-reactive regions in macaque monkey striate cortex. Cereb Cortex, 6:297-310.